

MODELLING MEASUREMENT PROCESSES IN COMPLEX SYSTEMS WITH PARTIAL DIFFERENTIAL EQUATIONS: FROM HEAT CONDUCTION TO THE HEART

MARKUS BÄR, STEFFEN BAUER, REGINE MODEL, RODRIGO WEBER DOS SANTOS

Department Mathematical Modeling and Data Analysis, Physikalisch-Technische Bundesanstalt (PTB), Abbestr. 2-12, 10587 Berlin, Germany.

The modelling of a measurement process necessary involves a mathematical formulation of the physical laws that link the desired quantity with the results of the measurement and control parameters. In simple cases, the measurement model is a functional relationship and can be applied straightforward. In many applications, however, the measurement model is given by partial differential equations that usually cannot be solved analytically. Then, numerical simulations and related tools such as inverse methods and linear stability analysis have to be employed. Here, we illustrate the use of partial differential equations for two different examples of increasing complexity. First, we consider the forward and inverse solution of a heat conduction problem in a layered geometry. In the second part, we show results on the integrative modelling of the heart beat which links the physiology of cardiac muscle cells with structural information on their orientation and geometrical arrangement.

1. Introduction

Analysing measurement processes in metrology requires often not only sophisticated tools of data analysis, but also numerical simulations of mathematical models and other computational tools. Here, we present a range of applications where the appropriate model is given by partial differential equations that can be solved only by numerical schemes like the methods of finite differences or finite elements. Mathematical models can serve different purposes; in the ideal case, the model is known exactly and simulations play the role of a „virtual experiment“. On the opposite side of the spectrum, models can also be used for developing hypotheses about observed behaviour in complicated systems and may serve as a guideline to design new experiments. Once plausible hypotheses have been established, models tend to evolve towards a more and more complete characterization of the system until the stage of the virtual experiment is reached. In the latter state, one may also employ inverse methods to obtain information on unknown physical parameters, functional dependencies or the detailed geometry of a measurement process from measurement data.

In this article, we illustrate the spectrum of possibilities of mathematical modelling by two examples. Section 2 describes finite element simulations of the heat equation and results of the inverse problem in a typical setup used for the measurement of heat conductivities as an example for a tractable virtual experiments. In Section 3, we will discuss basic aspects of the PTB heart modelling project. This project aims at the development of a „virtual organ” and may later serve as a normal in medical physics. Modelling results are crucial in the interpretation of electro- and magneto-cardiographic measurements. The philosophy of heart modelling is to build a complete model that integrates the physiology of heart muscles cells with the dynamic geometry of the heart. Then, one can predict the impact of molecular changes or pathologies on the propagation of potential waves in the heart muscle and ultimately on the form of the ECG or MCG. Such computations may be used for an improvement of the diagnosis of heart diseases. Along this line, we present results on modelling the ventricles of the mouse heart in a realistic three-dimensional geometry and with information on the fiber orientation.

2. Determination of Heat Conduction Parameters in Layered Systems

Within the process of development of new measurement procedures the part of mathematical modelling and simulation has gained importance in metrology. The so-called “virtual experiment” stands for the numerical simulation of an experiment based on a realistic mathematical model, virtual, because it proceeds in a computer instead in reality. Consequently, a virtual experiment design (VED) is a powerful numerical tool for: 1. the simulation, prediction, and validation of experiments; 2. optimization of measuring instruments, e.g., geometric design of sensors; 3. cause and effect analysis; 4. case studies, e.g., material dependencies; and 5. estimation of measurement errors.

For indirect measurement problems where the physical properties of interest have to be determined by measurement of related quantities a subsequent data analysis solves an inverse problem. Here, the virtual experiment works as a solver for the forward problem within the optimization procedure for the inverse problem. In this field, a proper example is given by the determination of thermal transport properties of materials under test - an important task in the fields of engineering which try to reduce the energy involved, e.g., in process engineering and in the building industry. As it is infeasible to directly measure the thermal conductivity λ and the thermal diffusivity α , the problem leads to an inverse heat transfer problem.

Non-steady-state methods such as the transient hot strip method (THS) [1-4] offer several advantages over conventional stationary methods, e.g., in shorter times of measurement and wider working temperature ranges. Here, a current-carrying thin metal strip is clamped between two sample halves where it simultaneously acts as a resistive heater and a temperature sensor. The transient temperature rise is calculated from measured voltage drop with the aid of the thermometer equation and yields the input information for the subsequent data analysis.

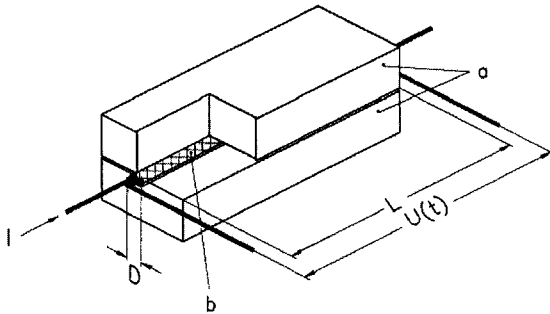


Figure 1. Transient hot strip: Thermal part of set-up. **a**, sample halves; **b**, hot-strip of width D and length L ; I , electric current; $U(t)$, THS voltage signal.

2.1 Mathematical Problem

In case of homogeneous media a well-posed inverse problem of parameter identification has to be solved using an analytic approximation solution for the heat conduction equation. More complicated is the situation for layered composites where no adequate analytic solution is at hand and, furthermore, the standard measurement situation violates the unique solvability [5]. It is known from experiments and theory that the set-up may be treated mathematically as a two-dimensional system if the strip is sufficiently long, i.e., $L \geq 100$ mm. In that case, heat losses at both ends are generally negligible. Therefore, the underlying three-dimensional model discussed so far can be limited to two spatial dimensions. Hence the problem may be defined in a cross sectional area perpendicular to the strip as shown for a two-layered sample in Figure 2.

2.2 Forward Problem

For symmetry reasons, the numerical integration domain can be reduced to a quarter of the cross sectional area. On the cut boundaries of the quadrant considered, homogeneous boundary conditions of the second kind are assumed, i.e., any heat flux vanishes. Then, for two concentric homogeneous layers the heat conduction equation is specified as

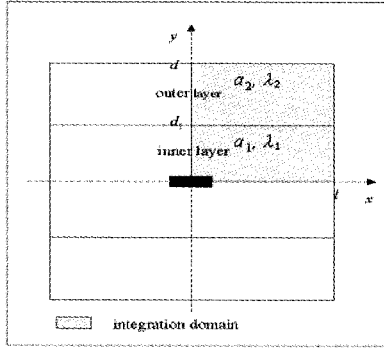


Figure 2. Schematic cross-section through the sample perpendicular to the strip. The thickness of the metal strip (0.01 mm) is exaggerated.

$$\rho c_p \frac{\partial T(x, y, t)}{\partial t} = \lambda(T_{xx}(x, y, t) + T_{yy}(x, y, t)) + q(x, y) \quad (1)$$

with the initial condition

$$T(x, y, 0) = T_0, \quad (x, y) \in \Omega_2 = [0, l] \times [0, d],$$

the boundary conditions of the third kind and the symmetry conditions

$$\begin{aligned} T_x(x, y, t) &= 0, & x=0, & 0 \leq y \leq d \\ T_y(x, y, t) &= 0, & 0 \leq x \leq l, & y=0. \end{aligned}$$

On the assumption of a negligible thermal contact resistance between the layers, the two additional conditions

$$\begin{aligned} T(x, d_1 - 0, t) &= T(x, d_1 + 0, t) \\ \lambda_1 T_y(x, d_1 - 0, t) &= \lambda_2 T_y(x, d_1 + 0, t) \end{aligned}$$

have to be satisfied. The half thickness of the whole specimen and its inner layer are denoted by d and d_1 , respectively; l is the half width of the specimen (see Figure 2).

The thermal diffusivity and the related volumetric heats of both layers are given by

$$\lambda = \begin{cases} \lambda_1, & 0 < y \leq d_1 \\ \lambda_2, & d_1 < y \leq d \end{cases} \quad \rho c_p = \begin{cases} \rho_1 c_{p1}, & 0 < y \leq d_1 \\ \rho_2 c_{p2}, & d_1 < y \leq d \end{cases}$$

where index 1 relates to the inner layer and index 2 to the outer layer. The thermal diffusivity a results from the known relation $a = \lambda / \rho c_p$. The heat source, q , is limited to the volume of the strip.

As an example, Figure 3 shows the finite-element simulation of the THS signals vs. $\ln t$ for a homogeneous and a two-layered sample applying a constant power of 1W to a strip of size $0.01 \times 3 \times 100 \text{ mm}^3$. The composite has an inner layer with thickness 20 mm and a outer layer with 220mm. Each signal is calculated for adiabatic and for isothermal boundary conditions. The curves representing the temperature rise for the two-layered sample may be divided into three characteristic regions. In the first region, the thermal properties of the inner core govern the temperature rise. Therefore, the curves of the two-layered and the homogeneous sample are in agreement. In the second region, the temperature rise of the metal strip is determined by the thermal conductivity and the thermal diffusivity of both the inner core and the outer layer. At the upper end of this region, the signals differ for adiabatic and isothermal conditions, respectively. Finally, in the third region, the additional influence of the surroundings becomes apparent.

2.3 Inverse Problem

The numerical simulation of the vector $T_{\text{sim}}(\lambda_1, \lambda, a_1, a, t)$ of the discrete measurement signal is the solution of the forward problem (1) for given thermal properties and a time vector t . In practice, the signal is a voltage drop. However, the relation to the temperature rise is defined by the linear thermometer equation. For comparison with simulated data the measurement data set is converted into a temperature vector T_{meas} . The related inverse problem of parameter identification

is formulated as an output-least squares problem

$$\begin{aligned} & \|T_{\text{sim}}(\lambda_1, \lambda_2, a_1, a_2, t) - T_{\text{meas}}(t)\|^2 \\ &= \sum_{i=1}^n |T_{i,\text{sim}}(\lambda_1, \lambda_2, a_1, a_2, t_i) - T_{i,\text{meas}}(t_i)|^2 = \sum_{i=1}^n F_i^2 = \min ! \end{aligned} \quad (2)$$

Here, n is the number of data points taken into account in the algorithm.

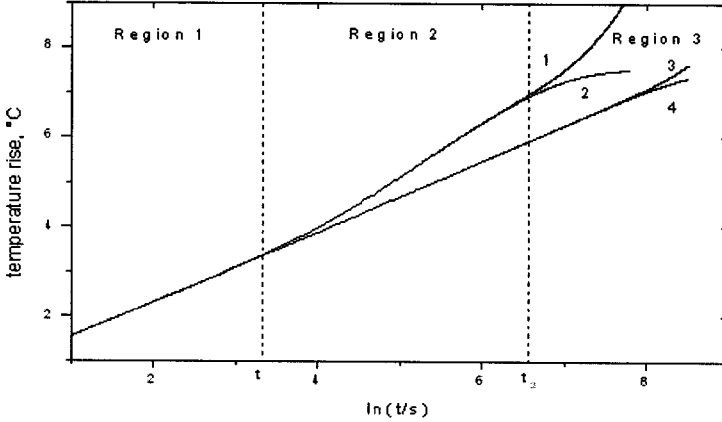


Figure 3. Numerical THS signal (temperature rise) for a layered sample (1-adiabatic, 2-isothermal) and a corresponding homogeneous sample (3-adiabatic, 4-isothermal).

With the identified $\lambda_1, a_1; \lambda_2, a_2$ the simulated signal T_{sim} is the best approximation to the experimental signal T_{meas} . (2) is solved by a modified Levenberg–Marquardt method [6]. The algorithm combines the Gauss–Newton method with the gradient method.

For layered composites, the subsequent determination of the parameters, beginning with the inner layer, strongly improves the condition of the problem. In the first step, a particular initial interval of the experimental signal is used for parameter identification of the inner layer and, in the following step, an adequately longer interval for the second layer. The time interval for the first step is reasonably chosen at $[0, t_1]$, see Figure 3. In the standard THS working regime the measurement time is less than t_2 , because here the boundary conditions have no bearing on the signal. However, in the second step the results for λ_2 and a_2 depend on the initial guess for the iteration procedure. Let us examine the error function E_i

$$E_t(\lambda, a) = \left\| T_{\text{sim}}(\lambda_1, \lambda, a_1, a, t) - T_{\text{sim}}(\lambda_1, \lambda_2, a_1, a_2, t) \right\|^2 \quad (3)$$

where the calculated vector $T_{\text{sim}}(\lambda_1, \lambda_2, a_1, a_2, t)$ acts as a measurement signal $T_{\text{meas}}(t)$, quasi as clean data without measurement uncertainty. The simulated vector function $T_{\text{sim}}(\lambda_1, \lambda, a_1, a, t)$ has two independent variables, the thermal conductivity and the thermal diffusivity of the second layer. Consequently, the error E_t is a two-dimensional function. Obviously, for $a = a_2$ and $\lambda = \lambda_2$, we obtain $E_t(\lambda_2, a_2) = 0$ (see Figure 4).

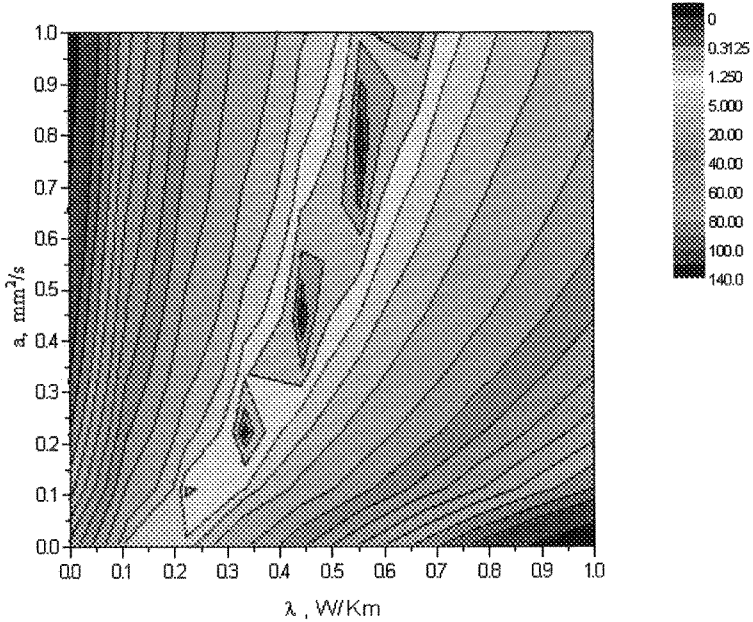


Figure 4. Error function $E_t(\lambda_2, a_2)$ for a measurement time of 300 s.

Furthermore, t_2 itself depends on the thermal transport properties where the influence of the thermal diffusivity a is much greater than for the thermal conductivity λ and in opposite direction. If t_{meas} is chosen to be sufficiently longer than t_2 , and if the boundary condition is known, a unique solution can be found in the second step. In the experimental situation, isothermal conditions may be better realized.

2.4 Summary

The algorithm for the determination of thermal conductivity and diffusivity of two-layered composites based on a finite-element model and an optimization strategy works in two steps: first the determination of the thermal properties of the inner layer, and second the same for the outer layer. The procedure has been successfully applied to the experimental THS signals derived from air bricks. Samples like these can be considered as composites of two parallel layers without any thermal contact resistance between them. In another test sample, a two-layered material made of polypropylene foam (inner layer) and polystyrene bulk material (outer layer) has been used as a model sample. Provided the measurement time is sufficiently long so that the THS signal contains information about the sample surface, the data analysis allows the thermal transport properties to be determined uniquely from THS signals.

3. Modeling Cardiac Electrophysiology

The heart as the center of the cardiovascular system is responsible to supply the body continuously with blood. The so called myocardium is a specialized muscular tissue which has self-excitable properties characterized by an action potential. Modeling of cardiac electrophysiology aims to calculate time and space distributions of potentials on the tissue and to get further data like simulated electro- or magnetocardiograms.

3.1 The Cardiac Action Potential

The origin of action potentials lies in the characteristics of the cell membrane. Within the membrane are several ion channels which are usually selective for one type of ion. In most cases the behaviour of an ion channel is voltage-dependent on the membrane potential. Membrane currents during the excitation phase can be described by systems of differential equations. An unexcited myocyte cell builds up an electrical potential difference of around $V_m = -89$ mV over the membrane. The total current through the membrane is the sum of the ionic currents and a capacitive current and leads directly to the Hodgkin-Huxley differential equation [7,8]:

$$C_m \frac{\partial V_m}{\partial t} = I_m - I_{ion}(V_m, \vec{g})$$

where C_m denotes the membrane capacity, I_{ion} is the sum of all currents through the different ionic channels, and I_m the membrane current.

3.2 Bidomain Models

The cardiac excitation is characterized by waves of depolarization which spread through the myocardium with propagation velocities ranging from 0.03 to 0.6 m/s. These waves are generated by the membrane currents and spread over the tissue by local currents through the intra- and extracellular domains. One needs thus to combine the above model of single cell excitation with a model for excitation spreading [9].

Cardiac cells are roughly cylindrical with a diameter of around 20 μm and a length of about 100 μm and are arranged in sheets of spatial differing orientation of these fibers. The electrical properties of the tissue are therefore quite anisotropic both for intra- and the extracellular space. Ohmic conductivities in three dimensions are then described by a conductivity tensor σ . The currents in both spaces are given by:

$$\vec{I}_{\text{ext}} = -\sigma_{\text{ext}} \nabla \phi_{\text{ext}}, \vec{I}_{\text{int}} = -\sigma_{\text{int}} \nabla \phi_{\text{int}}$$

The physiological source of currents in cardiac tissue are the transmembrane currents. Direction of this current is usually defined from inside to the outside of the cell. Conservation of total current flow then gives:

$$\nabla \vec{I}_{\text{ext}} = I_m, \nabla \vec{I}_{\text{int}} = -I_m$$

As the membrane currents consist of ionic and capacitive currents, we can write down now the complete bidomain equations:

$$C_m \frac{\partial V_m}{\partial t} = -\nabla(\sigma_{\text{ext}} \nabla \phi_{\text{ext}}) - I_{ion}(V_m, \vec{g})$$

$$C_m \frac{\partial V_m}{\partial t} = \nabla(\sigma_{\text{int}} \nabla \phi_{\text{int}}) - I_{ion}(V_m, \vec{g})$$

where $V_m = \phi_{\text{int}} - \phi_{\text{ext}}$ is the trans-membrane potential. For better numerical feasibility, the equations are usually rearranged to a parabolic and an elliptic PDE which can then be solved separately:

$$C_m \frac{\partial V_m}{\partial t} = \nabla (\sigma_{\text{int}} \nabla \phi_{\text{int}}) - I_{\text{ion}}(V_m, \vec{g})$$

$$\nabla (\sigma_{\text{int}} \nabla \phi_{\text{int}} + \sigma_{\text{ext}} \nabla \phi_{\text{ext}}) = 0$$

3.3 Example: Magnetocardiogram of the Mouse

During the design of a dedicated magnetocardiographic system used for measurements on mice, it was necessary to get an estimation of the maximum magnetic field strengths and magnetic field distribution in a realistic measurement geometry. A computer model based on the bidomain equations was used to fulfill these requirements of the design process.

The potentials were calculated on a finite element mesh consisting of $5 \cdot 10^5$ active nodes at a grid resolution of $250 \mu\text{m}$ describing the left and right ventricle (see Fig. 5). Solving of the bidomain equations is numerically quite complex. A semi-implicit Crank-Nicholson scheme combined with an algebraic multigrid preconditioner was used for the system of PDEs [10]. 100 ms simulated activity needed around 20 hours on a 16-processor 2.0 GHz opteron cluster.

The magnetic field was calculated by the Biot-Savart law from the superposition of intra- and extracellular cardiac tissue currents and volume currents through the surrounding medium:

$$\vec{I}_{\text{tot}} = \vec{I}_{\text{int}} + \vec{I}_{\text{ext}}$$

$$\vec{B} = \frac{\mu_0}{4\pi} \int_V \frac{\vec{I}_{\text{tot}} \times \vec{r}}{r^3} dV$$

The resulting magnetic field shows a maximum of 13 pT and a bipolar field distribution (see Fig. 6). It was therefore estimated that 6 SQUID magnetometers on a circumference around the mouse body should be sufficient to observe the bipolar and possible smaller multipolar parts of the overall magnetic field. Recent measurements on real mice could confirm these modeling results [11].

3.4 Summary

We described the basic physics of electrical propagation in the heart and showed some results of simulations of the mouse heart. Future work will continue using animal models like mice, rabbit and guinea pig in combination with experiments and drug testing issues. A mid-term goal is the implementation of a human heart model, which will require better hardware and further improvement of the numerical and mathematical methods used.

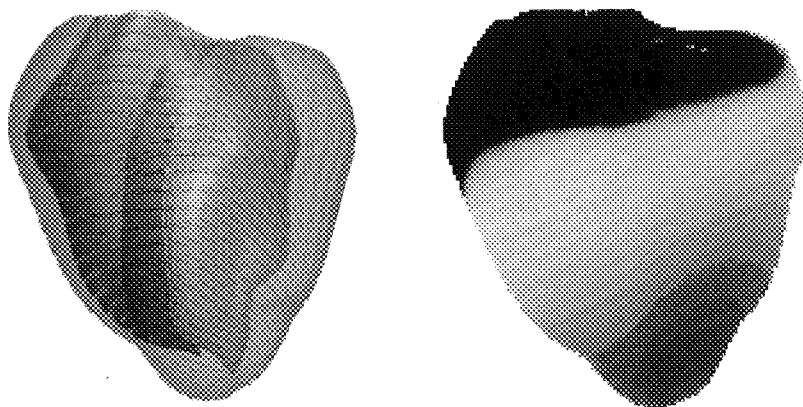


Figure 5. (a) Geometry and fiber orientations used for the mouse MCG simulation. Apex-base width of 7 mm. (b) Calculated transmembrane potential at $t = 15$ ms on the surface of the mouse heart mesh.

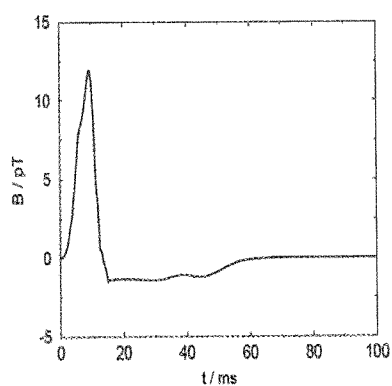
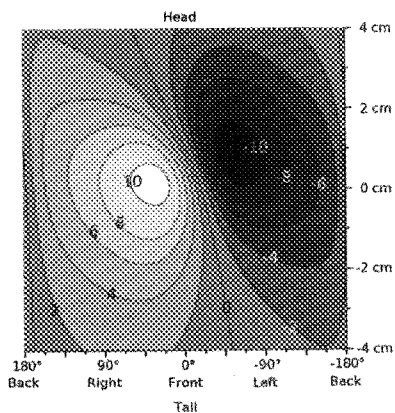


Figure 6. (a) Radial component of the calculated magnetic field at $\theta = -40^\circ$.



(b) Calculated distribution of the radial magnetic field during the maximum of QRS (field levels are given in units of pT).

4. Conclusion

We have exemplified the use of partial differential equations (PDEs) with the examples of heat conduction and cardiac propagation. Further application of PDE modelling in metrology are envisaged in the fields of non-imaging optics and bio-electromagnetism as well as in the rapidly developing field of modelling in biology and molecular medicine. Once the models are reasonably well characterized, solution of inverse problems can help in developing new measurement technology. A further challenge is the determination of uncertainties in situations where PDEs are employed.

References

1. S.E. Gustafsson *et al.*, Transient hot –strip method for simultaneously measuring thermal conductivity and thermal diffusivity of solids and fluids. *J. Phys. D* 12, 1411-1421 (1979).
2. K.D. Maglic, A. Cezairlyan, and V.E. Peletsky (eds), Compendium of thermophysical property measurement methods. Vol. 1: Survey of measurement techniques. Plenum Press, New York and London (1984).
3. U. Hammerschmidt, A linear procedure for analyzing transient hot strip signals. *Thermal Conductivity* 24, 123-134 (1999).
4. R. Model and U. Hammerschmidt, In *Advanced Computational Methods in Heat Transfer VI*, B. Suden, C.A. Brebbia (eds), WIT Press, Southampton, Boston, 407-416 (2000).
5. R. Model and U. Hammerschmidt, *High Temperature – High Pressure*, 34, 649-655, (2003).
6. Dennis, J.E. and Schnabel, R.B.: Numerical methods for unconstrained optimization and nonlinear equations. Prentice-Hall, Englewood Cliffs, N.J. (1983).
7. A. Panfilov, A. Holden (Editors), *Computational Biology of the Heart*, John Wiley & Sons, Chichester, 1997
8. G. T. Lines *et al.*, *Computing and Visualization in Science* 5(4):215-239 (2002).
9. E. Vigmond *et al.*, *IEEE Transactions on Biomedical Engineering*, 49, No. 11 (2002).
10. R. Weber dos Santos *et al.*, *IEEE Transactions on Biomedical Engineering*, 51, No. 11 (2004).
11. U. Steinhoff *et al.*, Contactless magnetocardiographic characterization of knock-out mice, accepted in *Folio Cardiologica* (2005)